12WCEE 2000

0224

EVALUATION OF LOCAL SITE EFFECTS IN THE KANTO DISTRICTBASED ON OBSERVATION RECORDS

Tetsushi KURITA[1], Midori KAWAHARA[2], Tadashi ANNAKA[3] And Satoru TAKAHASHI[4]

SUMMARY

The statistic attenuation relationships of acceleration response spectra are useful in the prediction of the intensity of seismic ground motion. For extremely accurate estimations, the consideration of local site effects is significant. Therefore, the local site effect was evaluated by using observed acceleration records of ground motion. The earthquake records database of the vertical array observation system was employed in order to investigate the characteristics of the seismic ground motion in the Kanto district, Japan. We consider an accurate evaluation of local site effects to be useful in the examination of the characteristics of ground motion, the prediction of ground motion, and so on. In this study, we evaluate the local site effects for ten vertical array observation sites in the Kanto district using the observation records.

INTRODUCTION

Tokyo Electric Power Company (TEPCO) has been constructing a database of earthquake observation records in order to investigate the characteristics of the seismic ground motion in the Kanto district, Japan. We consider an accurate evaluation of local site effects to be useful in the examination of the characteristics of ground motion, the prediction of ground motion, and so on. The objective of this study was to make an evaluation of the local site effects for ten vertical array observation sites in the Kanto district, based on the observation records.

The local site effect was considered to the geometric average of the acceleration response spectral ratio between the computed values from the statistic attenuation relations and observed seismic ground motions. It becomes possible to do the statistical analysis similar to this study by a large number of accumulation of seismic ground motion records. At the present time, TEPCO's database holds more than 17000 ground motion records. Then, it is considered that this data set is enough to do the statistic examination. The amplification factor of near-surface ground was obtained as the theoretical transfer function, which was calculated from the identified optimum ground structure model. The local site effects were compared with the amplification factors. From this investigation, it was understood that the local site effects can be explained by the one-dimensional SH amplification characteristics of surface geology.

LOCAL SITE EFFECT

The local site effects of seismic ground motion are expressed in terms of deviation from the average characteristics of seismic waves at the base layer. In this study, the average characteristics of seismic waves were calculated from the statistical attenuation relation of the acceleration response spectra. The response spectra obtained from observed records were then compared with the attenuation relations.

1.1 Attenuation Relation

The following attenuation model of the acceleration response spectrum, which was proposed by Annaka and Nozawa(1988), was employed in this study.

[1] *Seismic Engineering Department, Tokyo Electric Power Services Co., Ltd., Tokyo, Japan*
[2] *Seismic Engineering Department, Tokyo Electric Power Services Co., Ltd., Tokyo, Japan*
[3] *Seismic Engineering Department, Tokyo Electric Power Services Co., Ltd., Tokyo, Japan*
[4] *Power Engineering R&D Center, Tokyo Electric Power Company, Yokohama, Japan*

$$\log A(T) = Cm(T) \cdot M_J + Ch(T) \cdot H + Cd(T) \cdot \log D + Co(T) \quad (1a)$$

$$D = R + 0.35\exp(0.65M_J) \quad (1b)$$

in which T is the natural period, $A(T)$ is the acceleration response spectra, M_J is Japan Meteorological Agency magnitude, H is the depth of the center on the fault plane, and R is the closest distance to the fault plane, respectively. The regression coefficients of Eq. (1) are shown in Figure 1. The damping ratio of the response spectra is five per cent. This equation expresses the average intensity of ground motion at stiff ground (S-wave velocity is greater than 300 m/s) in the Kanto district. The population of multiple linear regression was obtained from TEPCO's database.

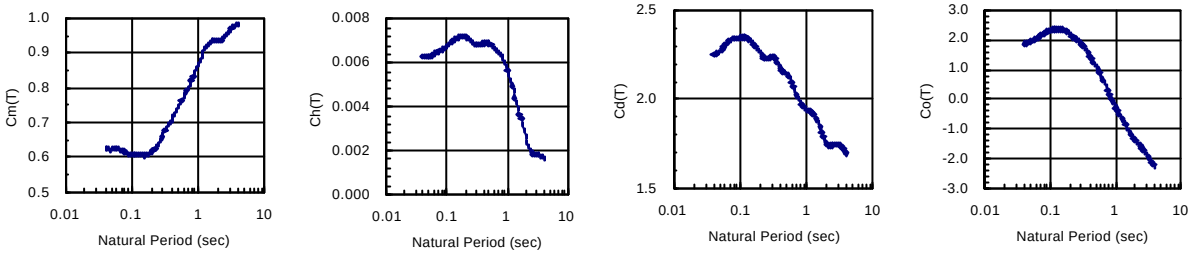

Figure 1 : Regression coefficients of attenuation equation of acceleration response spectra

Evaluation of Local Site Effect

The process of the calculation of local site effect (O/C) is displayed in Figure 2. The geometric average of response spectral ratios represents the local site effect (O/C).

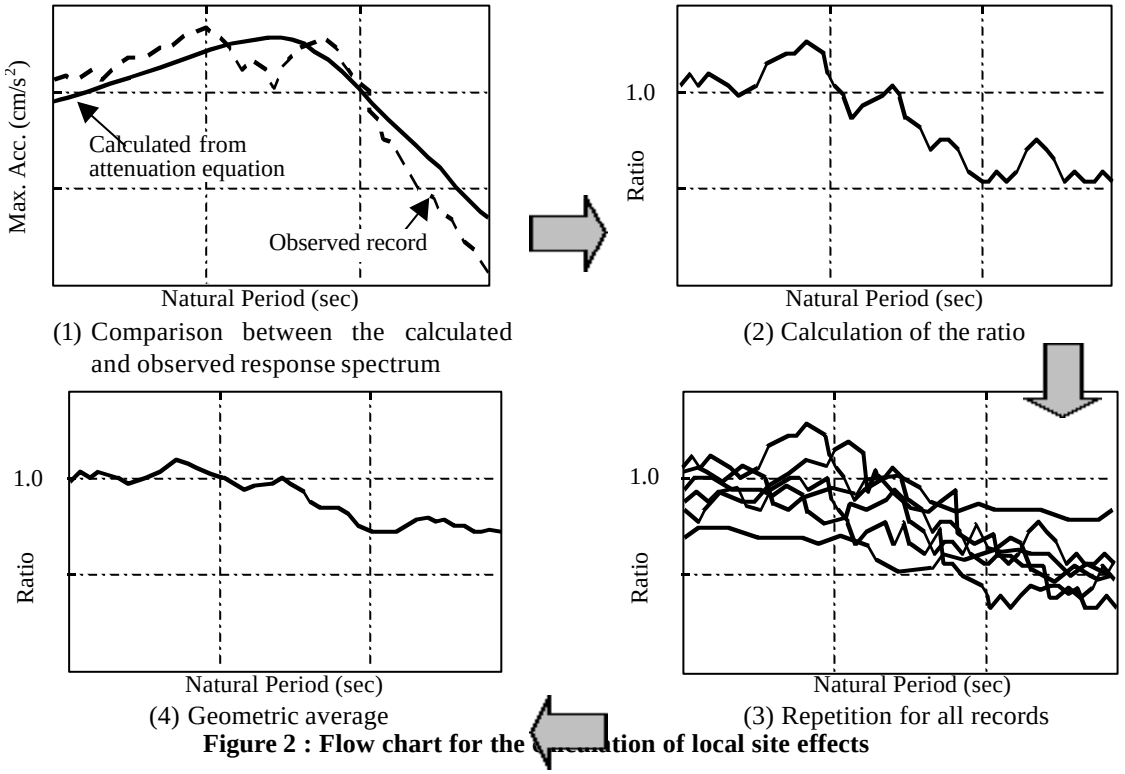

Figure 2 : Flow chart for the calculation of local site effects

2. GROUND AMPLIFICATION

Vertical Array Observation Sites

The distribution of the ten target sites in this study is indicated in Figure 3. The target sites are located around the Tokyo gulf in the Kanto district. The vertical array observation systems are installed at all sites. The arrangement of sensor locations is shown in Table 1.

Parameter Identification

The optimization theory was applied to parameter identification to obtain an optimum ground structure model (Kurita, 1997). The evaluation function is as follows:

$$\min . \quad \rightarrow \quad J = \frac{1}{2} \sum_{m=N_0}^{N_1} \sum_{i \in A} w_i \{ \ln R_i(w_m) - \ln H_i(w_m) \}^2 \tag{2}$$

in which $R_i(w_m); (i \in A)$ is the Fourier spectral ratio of the observation record, $H_i(w_m); (i \in A)$ is the theoretical transfer function, w_m is circular frequency, A is a set of Fourier spectral ratios, w_i is a weight factor, N_0 is a starting point of the analysis frequency range, and N_1 is an ending point for the analysis frequency range. In Eq. (2), the theoretical transfer function is obtained using the one-dimensional wave propagation theory. The Fourier spectral ratio can be calculated from observed records at boreholes. In this study, the following damping model was considered as the optimum ground structure model.

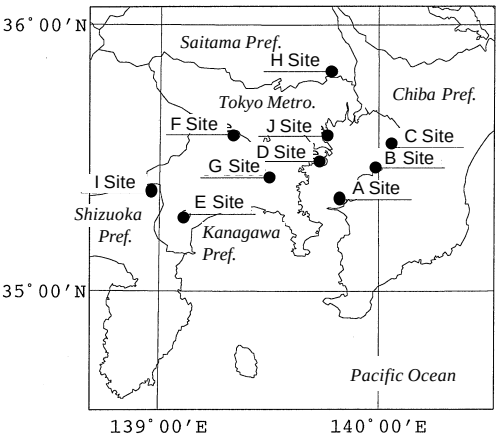

Figure 3 : Vertical array observation sites

$$h = a \cdot f^{b} \tag{3}$$

where h is the damping factor, f is the frequency, and a and b are coefficients. Eq. (3) can express the frequency-dependent damping factor (Kurita *et al*., 1996).

Optimum Ground Structure Models

The optimum ground structure models based on the parameter identification method are presented in Table 1. In this investigation, if anisotropic peak frequency appeared in the Fourier spectral ratios of observed records in two horizontal directions, two different models were evaluated each other. In Table 1, S-wave velocities and damping factors are the identified parameters. Thickness and densities are logging data. The transfer functions

Table 1 : Optimum Ground Structure Models

(1) A Site

a) X Direction

No.	Thickness (m)	Density (g/cm^3)	S-Wave Velocity (m/s)	Damping Factor ($h=a f^b$)		Soil Classification	Seismograph
				a	*b*		
1	9.8	1.78	149			Fill	*
2	4.2	1.70	235			Sand	
3	6.7	1.90	414	0.201	-0.548	Sand	
4	9.2	1.90	399			Sand	*
5	22.3	1.88	375			Sand	
6	-	1.93	445			Gravel	*

b) Y Direction

No.	Thickness (m)	Density (g/cm^3)	S-Wave Velocity (m/s)	Damping Factor ($h=a f^b$)		Soil Classification	Seismograph
				a	*b*		
1	9.8	1.78	145			Fill	*
2	4.2	1.70	225			Sand	
3	6.7	1.90	334	0.247	-0.696	Sand	
4	5.9	1.90	364			Sand	*
5	22.3	1.88	375			Sand	
6	-	1.93	445			Gravel	*

(2) B Site

No.	Thickness (m)	Density (g/cm^3)	S-Wave Velocity (m/s)	Damping Factor ($h=a f^b$)		Soil Classification	Seismograph
				a	*b*		
1	11.0	1.80	121			Clay	*
2	4.0	1.80	205			Sand	
3	1.5	1.80	369	0.095	-0.427	Sand	
4	5.2	1.70	237			Clay	*
5	10.5	1.85	272			Sand	
6	-	1.80	358			Clay	*

Table 1 : Optimum Ground Structure Models (continued)

(3) C Site

No.	Thickness (m)	Density (g/cm^3)	S-Wave Velocity (m/s)	Damping Factor ($h=a\,f^b$)		Soil Classification	Seismograph
				a	*b*		
1	4.3	1.80	101			Silty Fine Sand	*
2	2.8	1.90	172			Fine Sand	
3	4.6	1.90	207			Fine Sand	
4	4.0	1.73	148	0.158	-0.732	Silty Clay	
5	4.8	1.53	181			Tuffaceous Clay	
6	2.5	1.84	230			Fine Sand	
7	-	1.84	309			Silt	*

(4) D Site

No.	Thickness (m)	Density (g/cm^3)	S-Wave Velocity (m/s)	Damping Factor ($h=a\,f^b$)		Soil Classification	Seismograph
				a	*b*		
1	8.5	1.60	128			Fill	*
2	7.5	1.80	184			Sand	
3	16.0	1.55	165	0.114	-0.527	Clay	*
4	36.0	1.80	281			Clay	*
5	-	1.90	464			Sand	*

(5) E Site

No.	Thickness (m)	Density (g/cm^3)	S-Wave Velocity (m/s)	Damping Factor ($h=a\,f^b$)		Soil Classification	Seismograph
				a	*b*		
1	3.0	1.10	192			Loam	*
2	5.0	1.29	144			Loam	
3	6.0	1.45	260			Loam	
4	6.0	1.49	405	0.027	-0.010	Loam	
5	2.0	1.57	262			Loam	
6	3.0	1.67	704			Loam	
7	-	1.78	485			Agglomerate	*

(6) F Site

No.	Thickness (m)	Density (g/cm^3)	S-Wave Velocity (m/s)	Damping Factor ($h=a\,f^b$)		Soil Classification	Seismograph
				a	*b*		
1	6.0	1.35	193			Loam	*
2	4.0	1.45	221	0.107	-0.454	Loam	
3	6.0	1.51	253			Loam	
4	-	1.90	396			Clay	*

(7) G Site

No.	Thickness (m)	Density (g/cm^3)	S-Wave Velocity (m/s)	Damping Factor ($h=a\,f^b$)		Soil Classification	Seismograph
				a	*b*		
1	6.0	1.37	162			Loam	*
2	1.0	1.40	116			Loam	
3	3.0	1.50	216			Silt	
4	1.0	1.59	87			Silt	
5	10.0	1.61	278	0.147	-0.960	Silt	
6	2.0	2.29	465			Sand	
7	9.0	1.66	151			Silt	
8	2.0	1.68	187			Silt	
9	-	1.54	280			Silt	*

(8) H Site

a) X Direction

No.	Thickness (m)	Density (g/cm^3)	S-Wave Velocity (m/s)	Damping Factor ($h=a\,f^b$)		Soil Classification	Seismograph
				a	*b*		
1	4.0	1.74	91			Silt	*
2	10.7	1.74	188	0.216	-1.092	Silt	
3	-	1.65	321			Silt	*

b) Y Direction

No.	Thickness (m)	Density (g/cm^3)	S-Wave Velocity (m/s)	Damping Factor		Soil Classification	Seismograph
				a	*b*		
1	4.0	1.74	136			Silt	*
2	10.7	1.74	159	0.247	-0.875	Silt	
3	-	1.65	322			Silt	*

(9) I Site

a) NS Direction

No.	Thickness (m)	Density (g/cm^3)	S-Wave Velocity (m/s)	Damping Factor ($h=a\,f^b$)		Soil Classification	Seismograph
				a	*b*		
1	1.0	1.46	109			Scoria with Loam	*
2	4.0	1.46	129			Scoria with Loam	
3	2.0	1.48	110			Kuroboku Silt	
4	6.2	1.68	225	0.046	-0.162	Loam with Scoria	
5	3.8	1.69	375			Scoria with Loam	
6	7.0	1.69	529			Scoria with Loam	
7	-	1.95	823			Scoria	*

b) EW Direction

No.	Thickness (m)	Density (g/cm^3)	S-Wave Velocity (m/s)	Damping Factor ($h=a\,f^b$)		Soil Classification	Seismograph
				a	*b*		
1	1.0	1.46	102			Scoria with Loam	*
2	4.0	1.46	113			Scoria with Loam	
3	2.0	1.48	103			Kuroboku Silt	
4	6.2	1.68	205	0.069	-0.274	Loam with Scoria	
5	3.8	1.69	367			Scoria with Loam	
6	7.0	1.69	515			Scoria with Loam	
7	-	1.95	778			Scoria	*

Table 1 : Optimum Ground Structure Models (continued)

(10) J Site

No.	Thickness (m)	Density (g/cm^3)	S-Wave Velocity (m/s)	Damping Factor ($h=a\,f^b$)		Soil Classification	Seismograph
				a	*b*		
1	5.0	1.85	100			Fill	*
2	5.0	1.50	102			Clay	
3	4.0	1.80	153			Clay	
4	3.0	1.70	405			Sand	
5	5.0	1.60	226			Clay	
6	9.5	1.80	386	0.064	-0.245	Sand	*
7	1.5	1.80	517			Sand	
8	6.0	1.72	329			Clay	*
9	7.0	1.85	401			Sand	
10	16.0	1.85	349			Sand	
11	12.0	2.05	514			Gravel	
12	-	1.80	564			-	*

were calculated by using the one-dimensional SH wave propagation theory with optimum ground structure models. The one-dimensional transfer function was considered as an amplification characteristic of the surface geology.

RESULTS AND DISCUSSION

Figure 4 illustrates the comparison performed between the O/C of the acceleration response spectra and the amplification function of the surface geology. Only the horizontal components are considered. The upper graph of this figure shows the geometric average O/C of acceleration response spectra (solid line) and average $\pm$ one standard deviation (broken line). *N* means the number of data sets. The lower graph of the figure indicates a theoretical transfer function between the wave at ground surface and incident wave at the base layer. Evaluations of the local site effect of each site are as follows.

A Site: The O/C of the response spectra and the transfer functions are displayed within a frequency band ranging from 0.1 Hz to 25 Hz. However, the acceleration response spectrum converges to the peak ground motion in the high-frequency range. O/C could not provide information on the characteristics of seismic waves with respect to frequency in this range. Therefore, O/C above 10 Hz has been excluded from this investigation. The O/C of the response spectrum rise to the peak from 3 Hz to 4 Hz, while the theoretical transfer function dominates the same frequency band. Both peaks are about the same magnitude.

B Site: The primary peak of O/C appears from about 1 Hz to 2 Hz, and the secondary peak can be seen nearby 7 Hz to 8 Hz. The transfer function of the surface geology dominates much the same frequency band. Furthermore, the shapes of both spectra are in good agreement. However, the O/C is greater than the amplitude ratio of the transfer function.

C Site: A few differences can be recognized in the shape of the spectrum between the O/C and transfer function, while the both spectra dominate common frequencies at 2 Hz and 6Hz. The amplitude ratio of the transfer function at 6 Hz is more than two times. The O/C of response spectra at the same frequency is not particularly large. The two spectra are similar in overall form.

D Site: A gentle peak around 1 Hz and a steep peak at 4 Hz of O/C are in consistent with the theoretical transfer function. The absolute values of O/C are larger than the amplitude ratio of the transfer function.

E Site: Both spectra rise to peak from 3 Hz to 4 Hz. The ratios gradually increase with increasing frequency above this peak. The amplification factor of the transfer function at this peak frequency amounts to four times, while the O/C remains at two times.

F Site: A peak frequency at 4 Hz and the shape of O/C correspond to the ones for the transfer function. Furthermore, the ratios of both spectra at peak frequency are almost the same. However, the O/C of the response spectra is less than 1.0 at frequencies below 1.0 Hz. The cause of this phenomenon is obscure.

G Site: A primary peak from 3 Hz to 4 Hz and a secondary peak at 8 Hz can be recognized in both functions. The O/C of the response spectra is large, unlike than the amplitude ratio of the transfer function.

H Site: The X component of the transfer function is in conformity with the O/C of the response spectra. Both spectra increase with increasing frequency above 2 Hz. The Y component of the transfer function is different from the other two functions. The O/C is larger than the amplitude ratio of the transfer function.

I Site: The O/C and transfer functions are dominant at close to 3 Hz. At this site, it has been known that the Fourier spectra of observed records at ground surface peak at about 3 Hz. This characteristic of seismic waves can be explained by the amplification of the surface geology.

J Site: Both spectra rise to peak gently from 1 Hz to 2 Hz. The absolute value of O/C is in good agreement with the amplitude ratio of the transfer function.

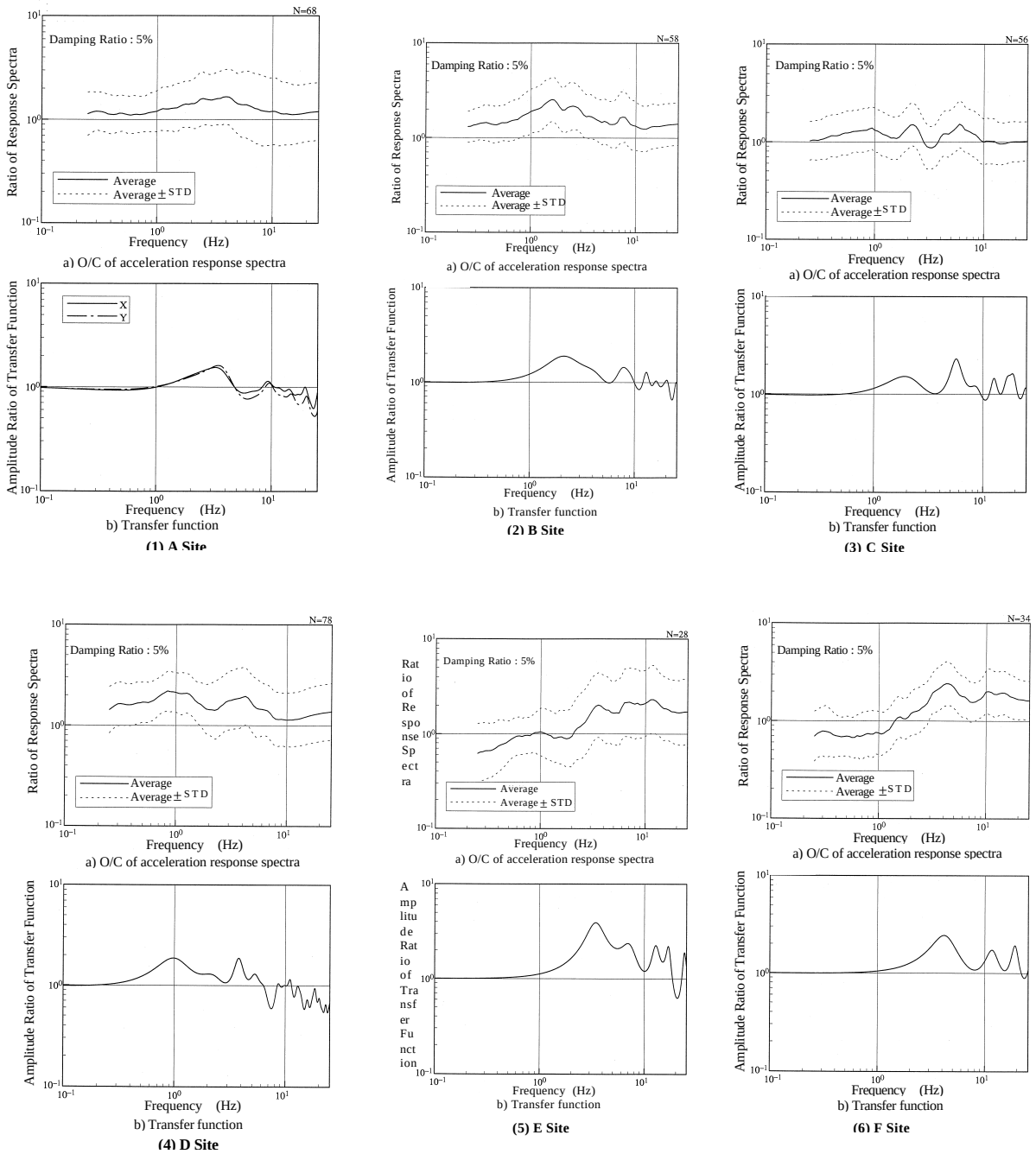

Figure 4 : Comparison between the O/C and amplification factor of surface geology

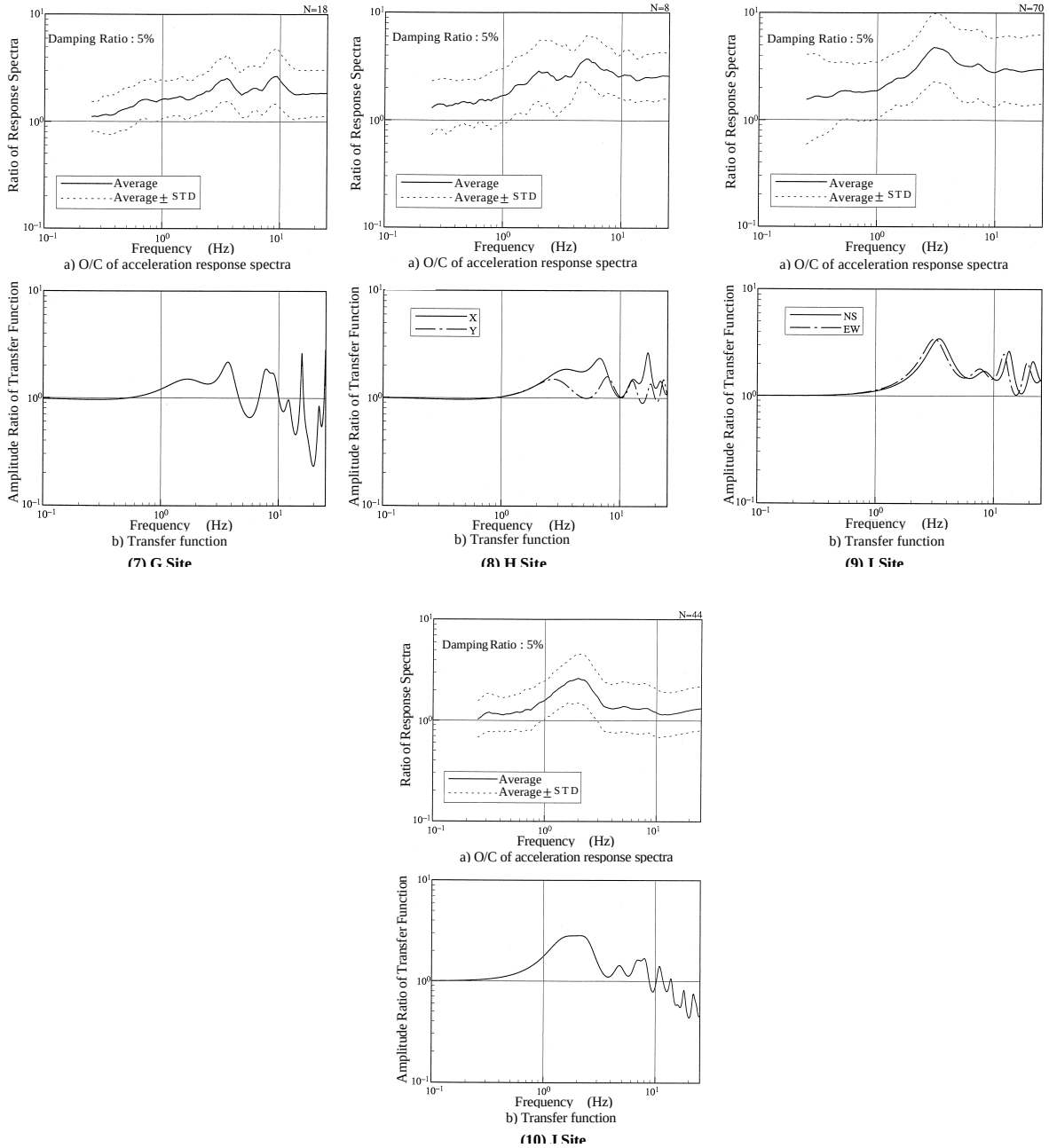

Figure 4 : Comparison between the O/C and amplification factor of surface geology (continued)

CONCLUSIONS

This paper deals with the evaluation of local site effects of seismic ground motions for vertical array sites in the Kanto district. Local site effect was calculated as the geometric average of the acceleration response spectral ratios between the estimated values from the attenuation relation and observed seismic ground motions. The amplification characteristic of surface geology was considered as the theoretical transfer function. A theoretical transfer function between the wave at ground surface and incident wave at the base layer was calculated from the optimum ground structure model. The optimum ground structure models were identified from vertical array observation records. Comparisons of the local site effect and the amplification factor were carried out. From

these examinations, a lot of local site effects can be explained by the one-dimensional SH amplification functions of the surface geology. However, several site effects cannot be elucidated by the amplification factors of surface geology. It is assumed that the irregular deep underground structure influences on these local site effects. We plan to extend the investigation into the effects of deep underground structure on seismic ground motions.

REFERENCES

Annaka, T. and Nozawa, Y. (1988), "A probabilistic model for seismic hazard estimation in the Kanto district", *Proceedings of Ninth World Conference on Earthquake Engineering*, 2, pp.107-112.

Kurita, T. (1997), "Dynamic characteristics of soil deposits identified from seismic records", *Transactions of the 14th International Conference on Structural Mechanics in Reactor Technology*, 7, pp.91-98.

Kurita, T., Tsuzuki, T., Annaka, T., Shimada, M. and Fujitani, M. (1996), "Scattering attenuation of seismic waves in inhomogeneous media", *Proceedings of Eleventh World Conference on Earthquake Engineering*